sustainability

MDPI

Article

Spatial and Temporal Variations in Extreme Precipitation and Temperature Events in the Beijing–Tianjin–Hebei Region of China over the Past Six Decades

Runze Tong [1], Wenchao Sun [1,*], Quan Han [1], Jingshan Yu [1] and Zaifeng Tian [2]

[1] Beijing Key Laboratory of Urban Hydrological Cycle and Sponge City Technology, College of Water Sciences, Beijing Normal University, Beijing 100875, China; 201721470023@mail.bnu.edu.cn (R.T.); 201831470017@mail.bnu.edu.cn (Q.H.); jingshan@bnu.edu.cn (J.Y.)

[2] Hebei Provincial Laboratory of Water Environmental Science, Hebei Provincial Academy of Environmental Science, Shijiazhuang 050051, China; zaifeng.tian@gmail.com

* Correspondence: sunny@bnu.edu.cn; Tel.: +86-10-5880-2736

Received: 27 December 2019; Accepted: 11 February 2020; Published: 14 February 2020

Abstract: Extreme weather events can cause a lot of damage in highly populated regions, such as in the Beijing–Tianjin–Hebei Region (BTHR) in northern China. To understand where and how extreme precipitation and temperature events are changing within the BTHR, data for 1959–2018 from 25 mereological stations were used to detect trends in the intensity, frequency, and duration of these events. The results showed that intensity, accumulated amount, the duration of extreme precipitation events, and the annual number of days with precipitation greater than 50 mm decreased on a regional scale over this 60-year period. Changes in extreme precipitation events at most stations were not statistically significant, although a few stations had a significant downward trend. The combined effects of the East Asian summer monsoon and rapid urbanization are possible reasons for these trends. Both the annual maximum and minimum temperature increased on a regional and local scale. The frequency of extreme hot and cold weather also, respectively, increased and decreased, with consistent patterns on a regional and local scale. However, the spatial changes of these trends were different, reflecting the effects of irrigation and urbanization on the regional surface energy balance. These findings are valuable to decisionmakers involved in disaster prevention in the BTHR and in other highly populated regions worldwide.

Keywords: Beijing–Tianjin–Hebei region; extreme temperature event; extreme precipitation event; temporal trends

1. Introduction

Extreme precipitation and temperature events can cause an enormous loss of human life, economic losses, and the loss of natural systems [1–3], and these issues have garnered attention worldwide in recent years [4]. Regarding extreme precipitation events, precipitation of a very high intensity, or long-lasting precipitation, can result in disastrous situations [5]. Heatwaves and cold air outbreaks are the extreme temperature events that have the greatest influence [6]. Many studies have shown that the global climate is undergoing significant changes that greatly influence both extreme precipitation and temperature events [7,8]. However, the changes in these events have high spatial heterogeneity in different regions [9–11]. Understanding the spatial and temporal variations in the intensity, frequency, and duration of extreme precipitation and temperature events on a regional scale is very important

for developing effective and appropriate countermeasures against possible damage caused by such extreme events [12–14].

The Beijing–Tianjin–Hebei Region (BTHR) is highly influenced by extreme climate events [15]. It is one of the most important and highly populated regions in China because it includes the capital of China (Beijing), a province-level municipality (Tianjin), and the province adjacent to Beijing and Tianjin (Hebei). Consistent with rapid social economic development and climate change, these areas have faced serious water scarcity, which has been increasing over the last 50 years [16]. From 1961 to 2010, the area was afflicted by varying degrees of drought, and drought occurred fairly frequently in the northeast and central parts of Hebei [17]. Social development and a high population density have contributed to the BTHR being vulnerable to extreme climate events.

As one of the most densely populated regions in China, and even worldwide, the BTHR has become a focus of study in terms of its characteristics of extreme precipitation and temperature events. Zhang et al. have explored the urbanization impact on summer precipitation in the BTHR by selecting one extremely dry year and one rainy year (1994 and 1997, respectively). The potential sensitivity of summer precipitation to urbanization under different climate conditions was also revealed [18]. Zhao et al. have investigated the temporal and spatial features of precipitation in the BTHR using observational data for 1965–2014 [19]. Zhang et al. have observed changes in extreme temperature events at eight meteorological stations in the BTHR [20]. Clearly, considering the rapid development occurring in the BTHR, a comprehensive examination of temporal trends in extreme precipitation and temperature events and their spatial heterogeneities using up-to-date and long-term observations is necessary to formulate adaptive strategies for extreme climate events.

With these requirements in mind, the objective of this study was to explore the long-term spatiotemporal changes in extreme precipitation and temperature events in the BTHR, using daily observational data from 25 meteorological stations from 1959–2018 for 17 indices representing the intensity and frequency of extreme precipitation events, as well as extremely high- and low-temperature events. The knowledge gained from this study is expected to provide valuable information for water resource management, as well as for drought and flood prevention, in this highly populated region and in similar semiarid regions worldwide.

2. Data and Methods

2.1. Study Area

The BTHR is located on the North China Plain, mostly within the Haihe River Basin (Figure 1). It includes Beijing and Tianjin, as well as 11 other major cities in Hebei (i.e., Baoding, Tangshan, Shijiazhuang, Langfang, Qinhuangdao, Zhangjiakou, Chengde, Changzhou, Hengshui, Xingtai, and Handan). The BTHR is the largest economic region in northern China, with a total area of 218,000 km^2 and a resident population of 110 million people. The topography is complex, with a high-altitude region in the northwest and a low-altitude region in the southeast. Belonging to the warm temperate continental monsoon climate, the BTHR has four distinct seasons, with hot, dry summers and cold, dry winters. Figure 2 shows that the BTHR is dominated by cropland, followed by forest and urban land cover.

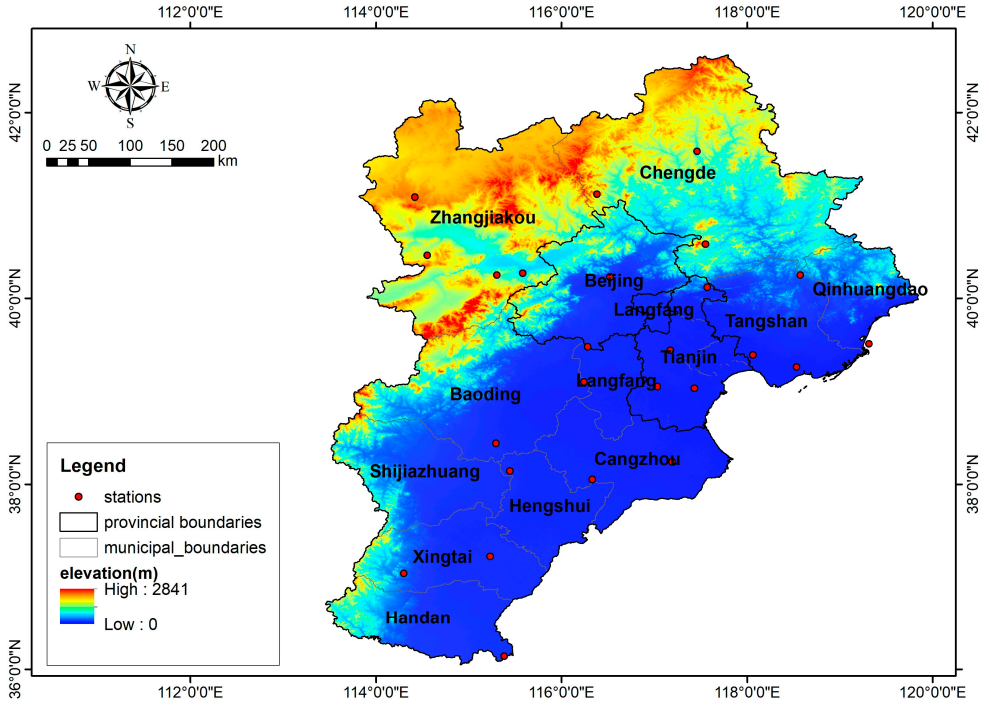

Figure 1. Topography of the Beijing–Tianjin–Hebei Region (BTHR) in China, showing the meteorological stations used in this study.

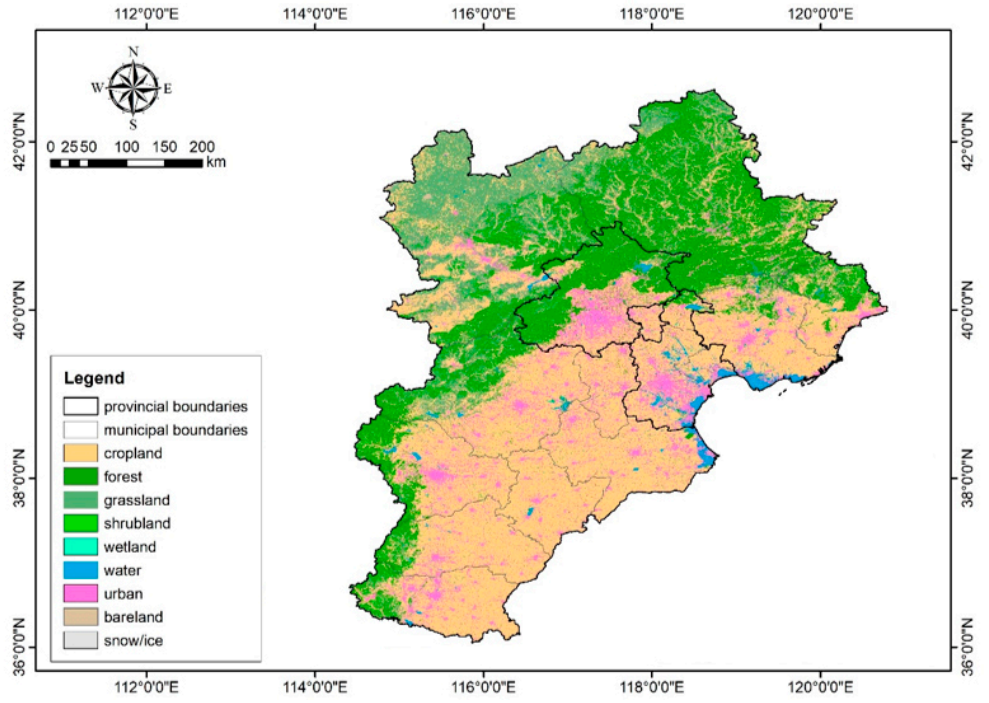

Figure 2. A land cover map of the Beijing–Tianjin–Hebei Region in China (derived from Moderate-Resolution Imaging Spectroradiometer data (2017)).

2.2. Data

Daily temperature and precipitation records for the period 1959 to 2018 (from 25 meteorological stations) were used in this study. The locations of these stations are shown in Figure 1. The temperature and precipitation data were obtained from the China Surface Climate Data Daily Dataset (V3.0) of the National Meteorological Information Center (http://data.cma.cn/). The selected meteorological

stations represented all of the typical terrain types in the BTHR, i.e., there were six stations located in the mountainous region and two stations located in the coastal region, and the remaining stations were located on the plain.

2.3. Methodology

2.3.1. Extreme Precipitation and Temperature Indices

Nine indices were used in this study to evaluate the temporal trends in extreme precipitation events (Table 1). Five indices characterized the property of intensity: these included annual average daily precipitation on wet days (SDII), annual maximum daily precipitation (RX1DAY), annual maximum consecutive 5-day precipitation (RX5DAY), annual total precipitation when daily precipitation was >the 95th percentile (R95P), and annual total precipitation when daily precipitation was >the 99th percentile (R99P). Four indices reflected frequency and duration: these included an annual count of days when daily precipitation was >10 mm (R10mm), an annual count of days when daily precipitation was >20 mm (R20mm), an annual count of days when daily precipitation was >50 mm (R50mm), and the maximum number of consecutive wet days (CWDs). Eight indices were applied to evaluate the temporal trends in extreme temperature events (Table 2). Four indices reflected the characteristics of hot weather: the annual daily maximum temperature (TMAX), the annual count of days when TMAX was >the 90th percentile (TX90P), the annual count of days when TMAX was >25 °C (SU25), and the annual count of days when the daily minimum temperature was >20 °C (TR20). Meanwhile, four other indices reflected the characteristics of cold weather: the annual minimum temperature (TMIN), the annual count of days when TMIN was <the 10th percentile (TN10P), the annual count of days when TMAX was <0 °C (FD0), and the annual count of days when TMIN was <0 °C (ID0). All indices were computed using RClimDex software [21–23].

Table 1. Definitions of the extreme precipitation event indices used in this study.

Index	Category	Definition	Units
SDII	intensity	annual average daily precipitation on wet days	mm
RX1DAY	intensity	annual maximum daily precipitation	mm
RX5DAY	intensity	annual maximum consecutive 5-day precipitation	mm
R95P	intensity	annual total precipitation when daily precipitation >the 95th percentile of daily precipitation in the 60-year period	mm
R99P	intensity	annual total precipitation when daily precipitation >the 99th percentile of daily precipitation in the 60-year period	mm
R10mm	frequency	annual count of days when daily precipitation >10mm	days
R20mm	frequency	annual count of days when daily precipitation >20mm	days
R50mm	frequency	annual count of days when daily precipitation >50mm	days
CWD	duration	maximum number of consecutive wet days	days

Table 2. Definitions of the extreme temperature event indices used in this study.

Index	Category	Definition	Units
TMAX	hot weather	annual daily maximum temperature	°C
TX90P	hot weather	annual count of days when TMAX >the 90th percentile of daily TMAX in the 60-year period	days
SU25	hot weather	annual count of days when TMAX >25 °C	days
TR20	hot weather	annual count of days when TMIN >20 °C	days
TMIN	cold weather	annual minimum temperature	°C
TN10P	cold weather	annual count of days when TMIN <the 10th percentile of daily TMIN in the 60-year period	days
FD0	cold weather	annual count of days when TMIN <0 °C	days
ID0	cold weather	annual count of days when TMAX <0 °C	days

2.3.2. Trend Analysis Method

The Mann–Kendall test was used to analyze the monotonic trend of changes in extreme temperature and precipitation events for the period 1959–2018 in the BTHR during the research process. The Mann–Kendall trend test has been widely used for the analysis of climate tendencies in recent years [24–26]. The advantage of this test is that assumptions about the form of the data distribution are no longer required. It can detect more significant trends than can methods based on assumptions about data distribution (when it is applied to annual precipitation series) [27]. For the time series data $X = \{x_1, x_2, \ldots, x_n\}$ (where n is the length of the time series), the test statistic S is computed as

$$S = \sum_{j=1}^{n-1} \sum_{k=j+1}^{n} sgn(x_k - x_j), \tag{1}$$

where

$$sgn(x_k - x_j) = \begin{cases} 1, x_k - x_j > 0 \\ 0, x_k - x_j = 0 \\ -1, x_k - x_j < 0 \end{cases}. \tag{2}$$

Here, x_j and x_k are defined as the measured annual values of j and k ($k > j$). The mean and variance of S are computed as follows based on the assumption that there is an independent and identical distribution of data:

$$\mathrm{E(S)} = 0, \tag{3}$$

$$VAR(S) = n(n-1)(2n-15)/18. \tag{4}$$

Considering the existing tied ranks (equal observations) in the data, the variance of S is updated to

$$VAR(S) = [n(n-1)(2n-15) - \sum_{i=1}^{m} t_i(t_i-1)(2t_i+5)]/18, \tag{5}$$

where m is the number of tied groups, and t_i is the number of datapoints in the ith tied group. When the sample size is >10, the standardized normal statistic Z is estimated as

$$Z = \begin{cases} \frac{S-1}{\sqrt{VAR(S)}}, S > 0 \\ 0, S = 0 \\ \frac{S+1}{\sqrt{VAR(S)}}, S < 0 \end{cases}. \tag{6}$$

In this study, a trend was regarded as being statistically significant at the 0.05 level, i.e., if $|Z|>$ 1.96, the null hypothesis of having no trend would be rejected. Where there is a significant trend ($p <$

0.05), the magnitude of changes per year can be computed using Sen's slope estimator [28]. The slope is calculated as

$$\theta = \text{Median}\left(\frac{x_j - x_i}{j - i}\right), i < j, \quad (7)$$

where $\theta > 0$ indicates an upward trend, and $\theta < 0$ indicates a downward trend.

3. Results

3.1. Trends of Extreme Precipitation Events on a Regional Scale

Figure 3 and Table 3 show time series for five indices representing the intensity of extreme precipitation events and trends on a regional scale. No significant trend was detected for SDII, which means that the daily precipitation intensity did not change significantly over the past six decades. However, the annual maximum one-day (RX1DAY) and five-day precipitation (RX5DAY) had a significant decreasing trend. R95P and R99P also were found to be descending, indicating that the accumulated amount of extreme precipitation within a year fell on a regional scale.

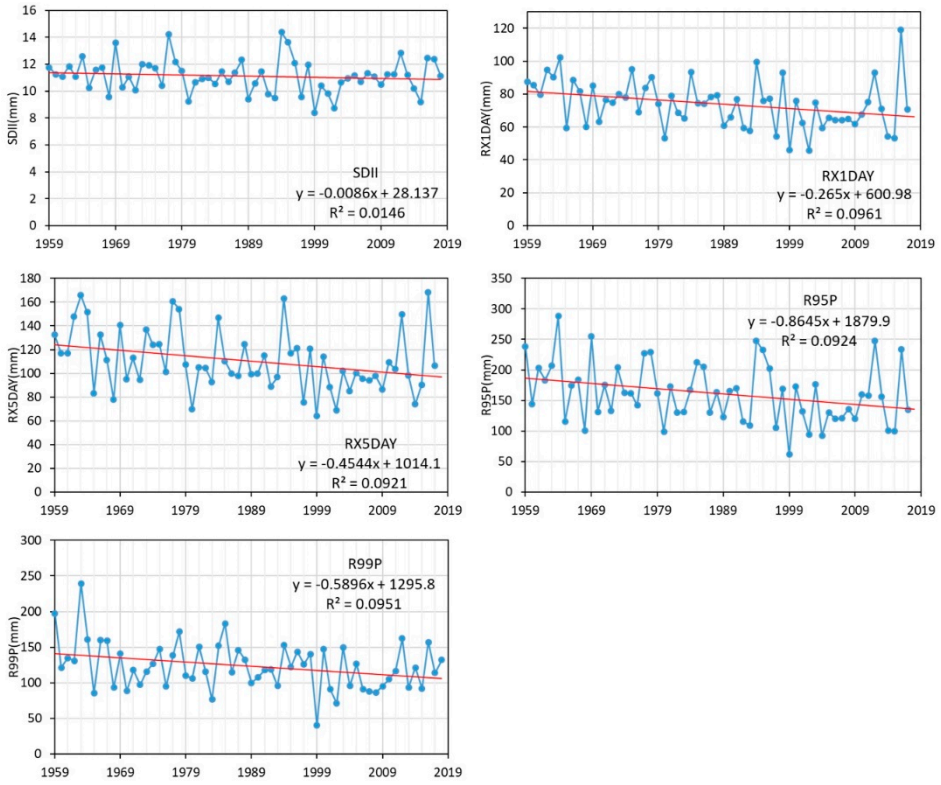

Figure 3. Region-averaging time series for indices indicating the intensity of extreme precipitation events in the Beijing–Tianjin–Hebei Region from 1959 to 2018. The straight red line represents the linear trend line for 1959–2018. NB (Nota Bene): SDII, the annual average daily precipitation on wet days; RX1DAY, the annual maximum daily precipitation; RX5DAY, the annual maximum consecutive five-day precipitation; R95P, the annual total precipitation when daily precipitation was >the 95th percentile of daily precipitation; and R99P, the annual total precipitation when daily precipitation was >the 99th percentile of daily precipitation.

Table 3. The trends of five indices indicating the intensity of extreme precipitation events in the Beijing–Tianjin–Hebei Region from 1959 to 2018.

Index	Average Value	Trend	Significant or Not
SDII	11.1mm	−0.086 mm/decade	No
RX1DAY	74.1 mm	−2.650 mm/decade	Yes
RX5DAY	110.7 mm	−4.544 mm/decade	Yes
R95P	161.3 mm	−8.645 mm/decade	Yes
R99P	132.1 mm	−5.896 mm/decade	Yes

NB: SDII, the annual average daily precipitation on wet days; RX1DAY, the annual maximum daily precipitation; RX5DAY, the annual maximum consecutive five-day precipitation; R95P, the annual total precipitation when daily precipitation was >the 95th percentile of daily precipitation; and R99P, the annual total precipitation when daily precipitation was >the 99th percentile of daily precipitation.

The time series characterizing the frequency and duration of extreme precipitation events and their trends are shown in Figure 4 and Table 4, respectively. No significant trends were detected for the number of days with precipitation greater than 10 mm or 20 mm. Meanwhile, both R50mm and CWD had significant decreasing trends, showing signs that the frequency and duration of extreme precipitation events have diminished in recent years.

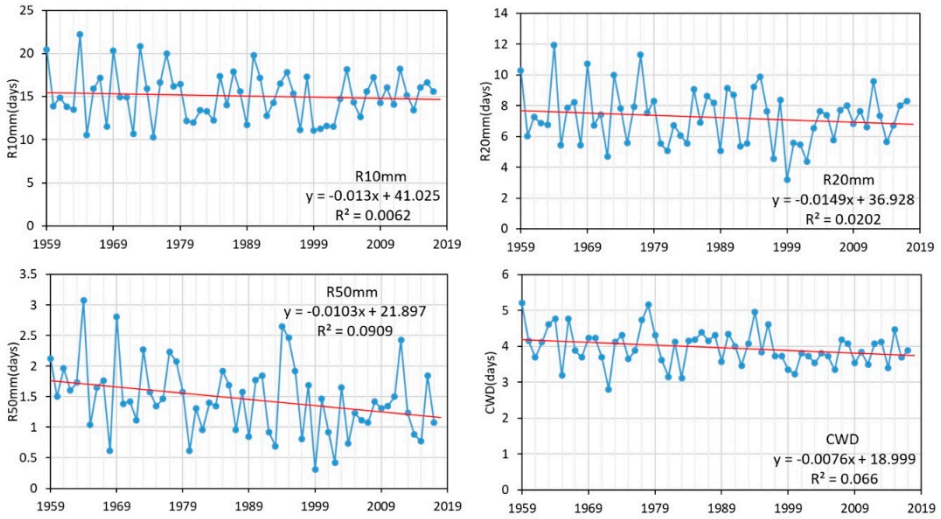

Figure 4. Region-averaging time series for indices indicating the frequency and duration of extreme precipitation events in the Beijing–Tianjin–Hebei region from 1959 to 2018. The red straight line represents the linear trend line for 1959–2018. NB: R10mm, the annual count of days when daily precipitation was >10 mm; R20mm, the annual count of days when daily precipitation was >20 mm; R50mm, the annual count of days when daily precipitation was >50 mm; and CWD, the maximum number of consecutive wet days.

Table 4. The detected trends of four indices indicating the frequency and duration of extreme precipitation events in the Beijing–Tianjin–Hebei Region from 1959 to 2018.

Index	Average Value	Trend	Significant or Not
R10mm	15.10 days	−0.130 days/decade	No
R20mm	7.25 days	−0.149 days/decade	No
R50mm	1.46 days	−0.103 days/decade	Yes
CWD	3.97 days	−0.076 days/decade	Yes

NB: R10mm, the annual count of days when daily precipitation was >10 mm; R20mm, the annual count of days when daily precipitation was >20 mm; R50mm, the annual count of days when daily precipitation was >50 mm; and CWD, the maximum number of consecutive wet days.

3.2. Spatial Distribution of Temporal Trends in Extreme Precipitation Events

The spatial distributions of the five indices related to the intensity of extreme precipitation events in the BTHR are shown in Figure 5. The trends at most stations were not statistically significant. For SDII, RX1DAY, and RX5DAY, only trends at one, two, and four stations were statistically significant: these stations were located west, south, and east of Beijing City and in Baoding City, respectively. When examining R95P and R99P, which quantified the annual accumulated amount of extreme precipitation events, it was found that only six and five stations, respectively, had significant decreasing trends, most of which also showed significant decreasing trends in SDII, RX1DAY, and RX5DAY. Trends for the indices characterizing the frequency of extreme precipitation events of different magnitudes (R10mm, R20mm, and R50mm) are shown in Figure 6. Only trends at one, two, and four stations were found to decrease significantly. Notably, the stations with significant trends were not consistent across the three indices. For CWD, the trends at almost all of the stations were not statistically significant.

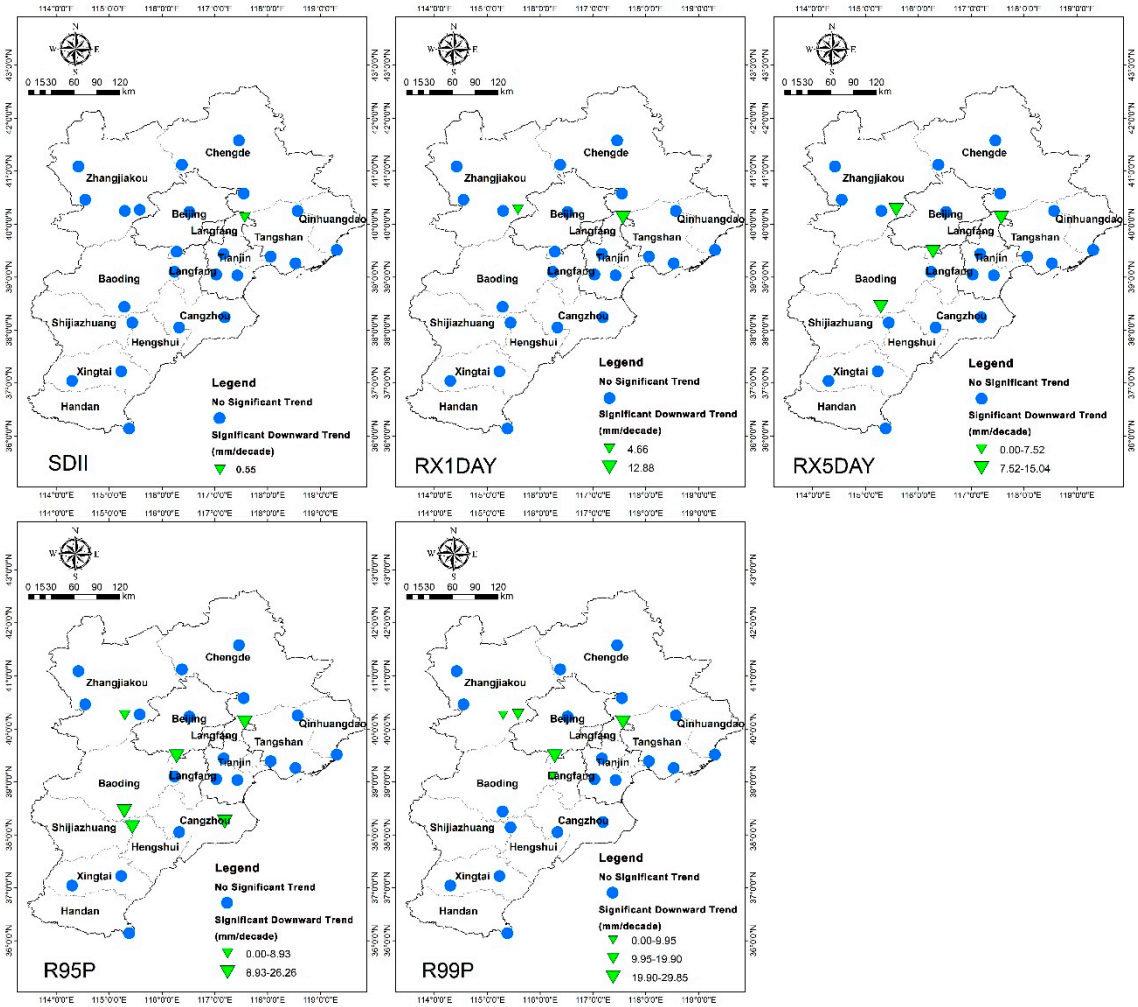

Figure 5. Spatial distributions of trends in indices representing the intensity of extreme precipitation events at the meteorological stations in the Beijing–Tianjin–Hebei Region from 1959 to 2018. NB: SDII, the annual average daily precipitation on wet days; RX1DAY, the annual maximum daily precipitation; RX5DAY, the annual maximum consecutive five-day precipitation; R95P, the annual total precipitation when daily precipitation was >the 95th percentile of daily precipitation; and R99P, the annual total precipitation when daily precipitation was >the 99th percentile of daily precipitation.

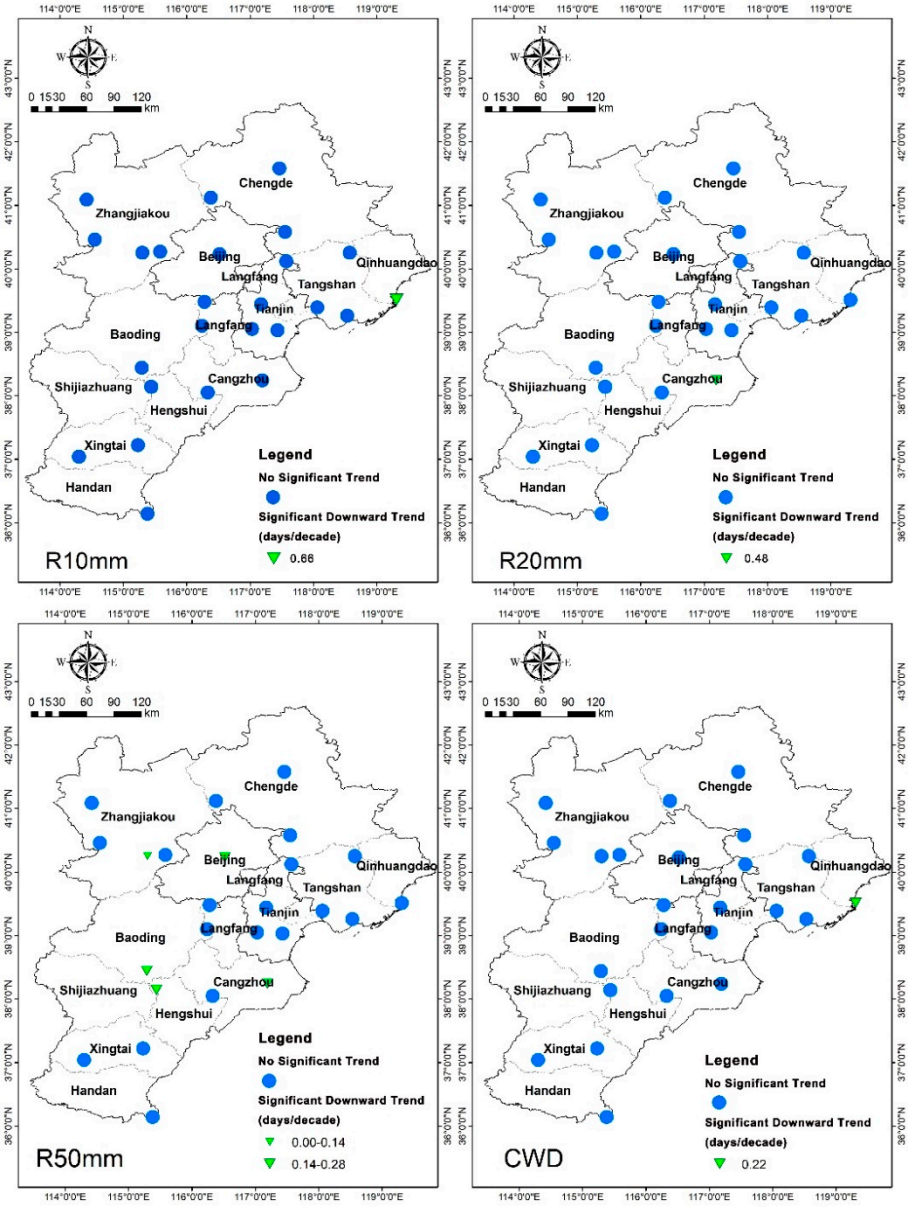

Figure 6. Spatial distributions of trends in indices representing the frequency and duration of extreme precipitation events for the meteorological stations in the Beijing–Tianjin–Hebei region from 1959 to 2018. NB: R10mm, the annual count of days when daily precipitation was >10 mm; R20mm, the annual count of days when daily precipitation was >20 mm; R50mm, the annual count of days when daily precipitation was >50 mm; and CWD, the maximum number of consecutive wet days.

3.3. Trends of Extreme Temperature Events on a Regional Scale

Time series for the four indices showing hot weather extreme events and their trends over the entire BTHR are shown in Figure 7 and Table 5. TMAX had a significant upward trend, with a magnitude of 0.198 °C/decade, giving a clear indication that daily maximum temperature increased. TX90P had a statistically significant increasing trend, suggesting that the number of days with extremely hot weather have increased in recent years. Significant increases were also detected for the two indices quantifying the number of days that the maximum and minimum daily temperatures were higher than 25 °C(SU25) and 20 °C (TR20), respectively.

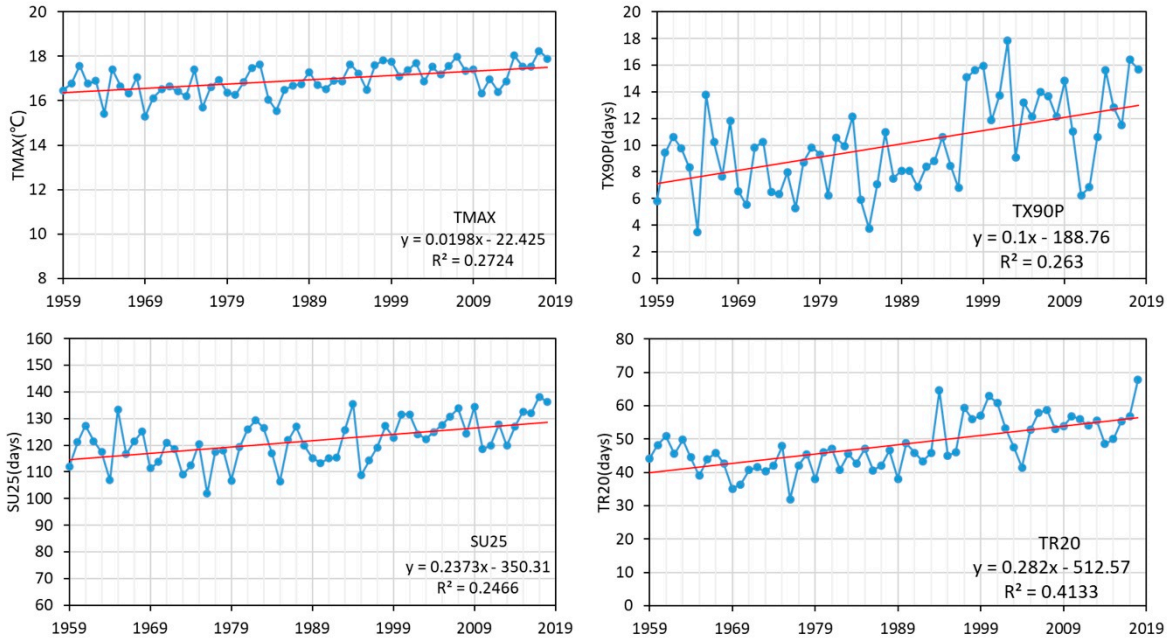

Figure 7. Region-averaging time series for indices indicating extreme hot weather events in the Beijing–Tianjin–Hebei Region from 1959 to 2018. The red straight line represents the linear trend line for 1959–2018. NB: TMAX, the maximum temperature; TX90P, the annual count of days when TMAX was >the 90th percentile; SU25, the annual count of days when TMAX was >25 °C; and TR20, the annual count of days when the daily minimum temperature was >20 °C.

Table 5. The trends of the four indices indicating extreme hot weather events in the Beijing–Tianjin–Hebei Region from 1959 to 2018.

Index	Average Value	Trend	Significant or Not
TMAX	16.93 °C	0.198 °C/decade	Yes
TX90P	10.04 days	1.000 days/decade	Yes
SU25	121.61 days	2.373 days/decade	Yes
TR20	48.24 days	2.820 days/decade	Yes

NB: TMAX, the maximum temperature; TX90P, the annual count of days when TMAX was >the 90th percentile; SU25, the annual count of days when TMAX was >25 °C; and TR20, the annual count of days when the daily minimum temperature was >20 °C.

Figure 8 and Table 6 show the trends for extreme cold temperature indices at a regional scale. TMIN had a significant increasing trend, with an increment (0.383 °C/decade) that was higher than that of TMAX (0.198 °C/decade). A significant decreasing trend was detected for TN10P, which quantified the number of days with an extremely low daily minimum temperature. In addition, ID0 and FD0 also had significant descending trends, suggesting that the numbers of days that the maximum and minimum daily temperatures were lower than 0 °C increased. All of these indices indicated that the magnitude and frequency of extremely low temperature events decreased.

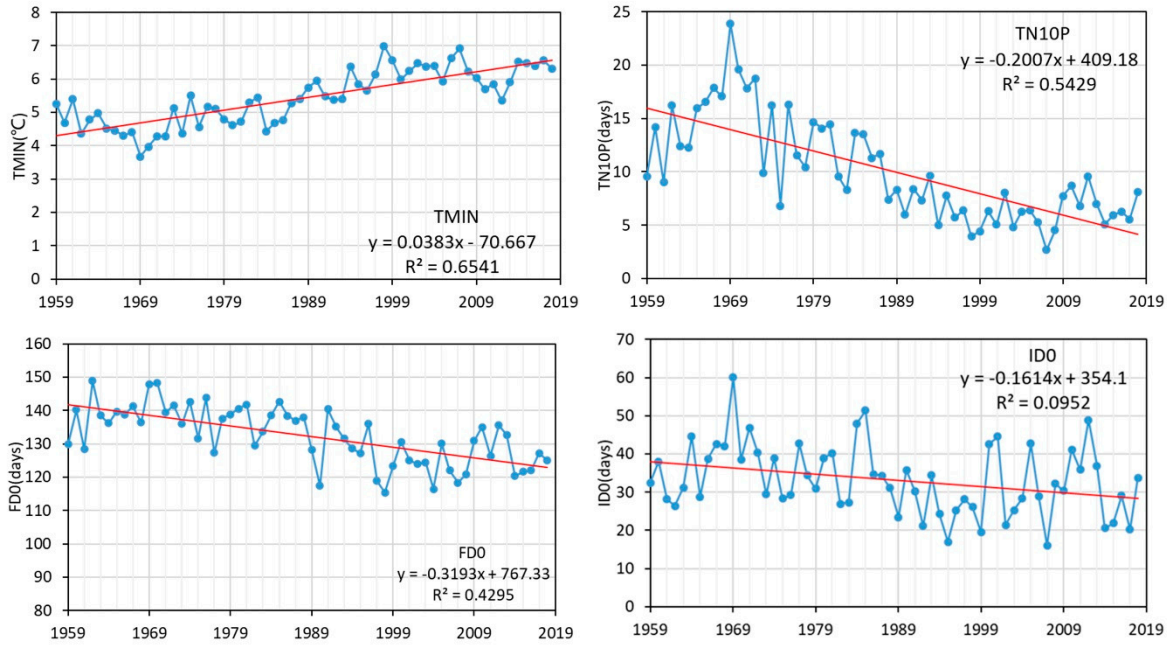

Figure 8. Region-averaging time series for indices indicating extreme cold weather events in the Beijing–Tianjin–Hebei Region from 1959 to 2018. The red straight line represents the linear trend line for 1959–2018. NB: TMIN, the annual minimum temperature; TN10P, the annual count of days when TMIN was <the 10th percentile; FD0, the annual count of days when TMAX was <0 °C; and ID0, the annual count of days when TMIN was <0 °C.

Table 6. The detected trends of four indices indicating extreme cold weather events in the Beijing–Tianjin–Hebei Region from 1959 to 2018.

Index	Average Value	Trend	Significant or Not
TMIN	5.44 °C	0.383 °C/decade	Yes
TN10P	10.08 days	−2.070 days/decade	Yes
FD0	132.41 days	−3.193 days/decade	Yes
ID0	33.23 days	−1.614 days/decade	Yes

NB: TMIN, the annual minimum temperature; TN10P, the annual count of days when TMIN was <the 10th percentile; FD0, the annual count of days when TMAX was <0 °C; and ID0, the annual count of days when TMIN was <0 °C.

3.4. Spatial Distribution of Temporal Trends during Extreme Temperature Events

The spatial patterns of trends in the indices indicating hot extreme temperature events are shown in Figure 9. TMAX had a significant increasing trend at most stations, except for four stations in the southern part of the BTHR, which showed nonsignificant changes. This indicates that in most areas of the BTHR, the daily maximum temperature increased. The spatial distribution of TX90P was very similar to that of TMAX, with only two stations having nonsignificant trends in the south. The number of days in a year that the maximum temperature was higher than 25 °C (SU25) rose significantly at most stations, although five stations in the south and two stations in the middle of the BTHR had trends that remained unchanged. For TR20, most stations had significant increases, although the locations of stations with nonsignificant changes were different from those listed above, as they were scattered throughout the north and east.

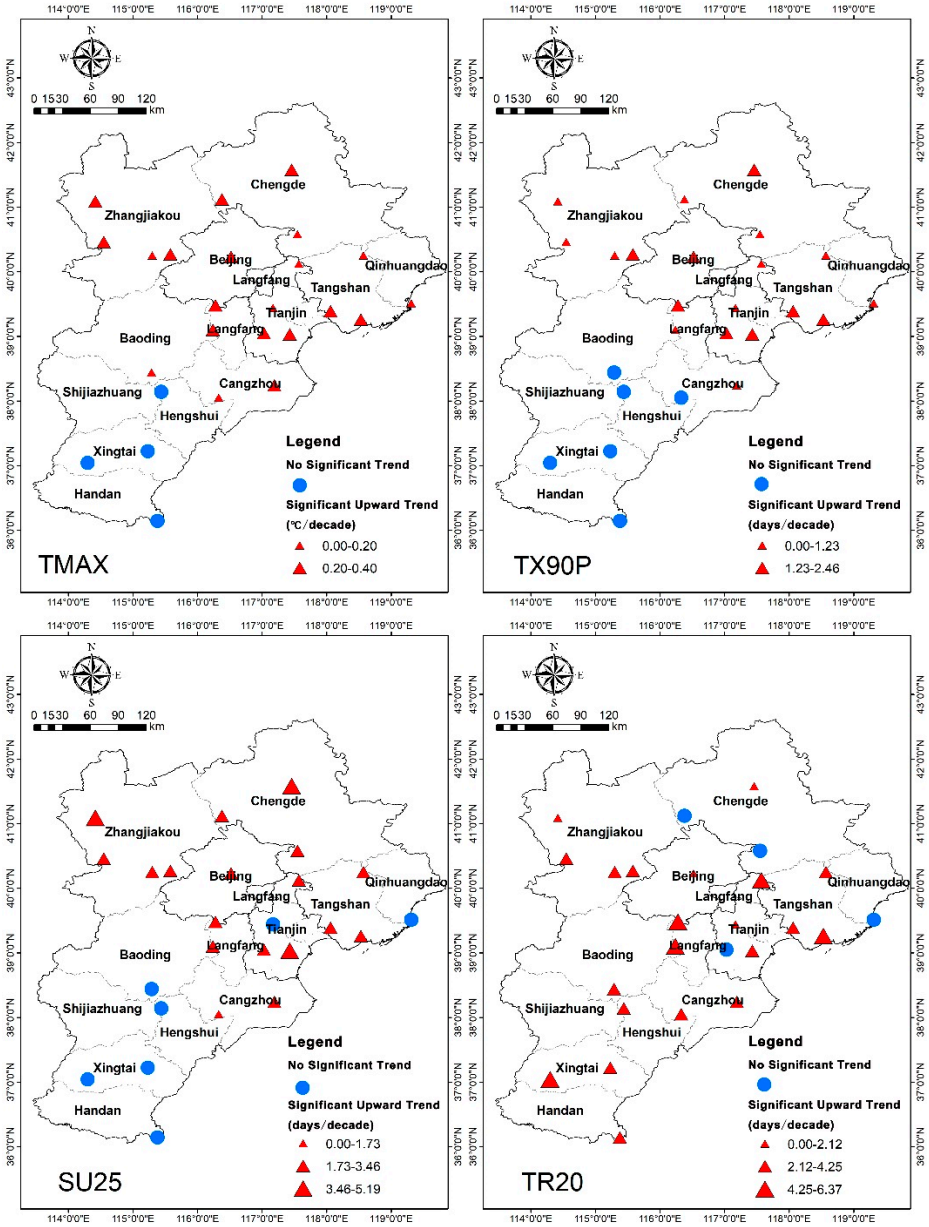

Figure 9. Spatial distributions of trends in indices representing hot weather extreme events for the meteorological stations in the Beijing–Tianjin–Hebei Region from 1959 to 2018. NB: TMAX, the maximum temperature; TX90P, the annual count of days when TMAX was >the 90th percentile; SU25, the annual count of days when TMAX was >25 °C; and TR20, the annual count of days when the daily minimum temperature was >20 °C.

Figure 10 shows the spatial distribution of trends in indices indicating cold extreme temperature events. For TMIN, most stations had upward trends, indicating that the daily minimum temperature rose. Significant downward trends in TN10P were detected at most stations, with three exceptions located in the north and east of the BTHR. More than half of the stations had an increasing trend for FD0 and ID0. However, the spatial patterns of the trends in these two indices were different. For FD0, the stations with significant increasing trends were spread over the whole region, while the five stations without significant trends were scattered in the center and northeast of the BTHR. For ID0, the stations exhibiting increasing trends were in the central part of the BTHR, including Beijing, Tianjin, Langfang, Tangshan, and Cangzhou, and in Zhangjiankou in the northwest.

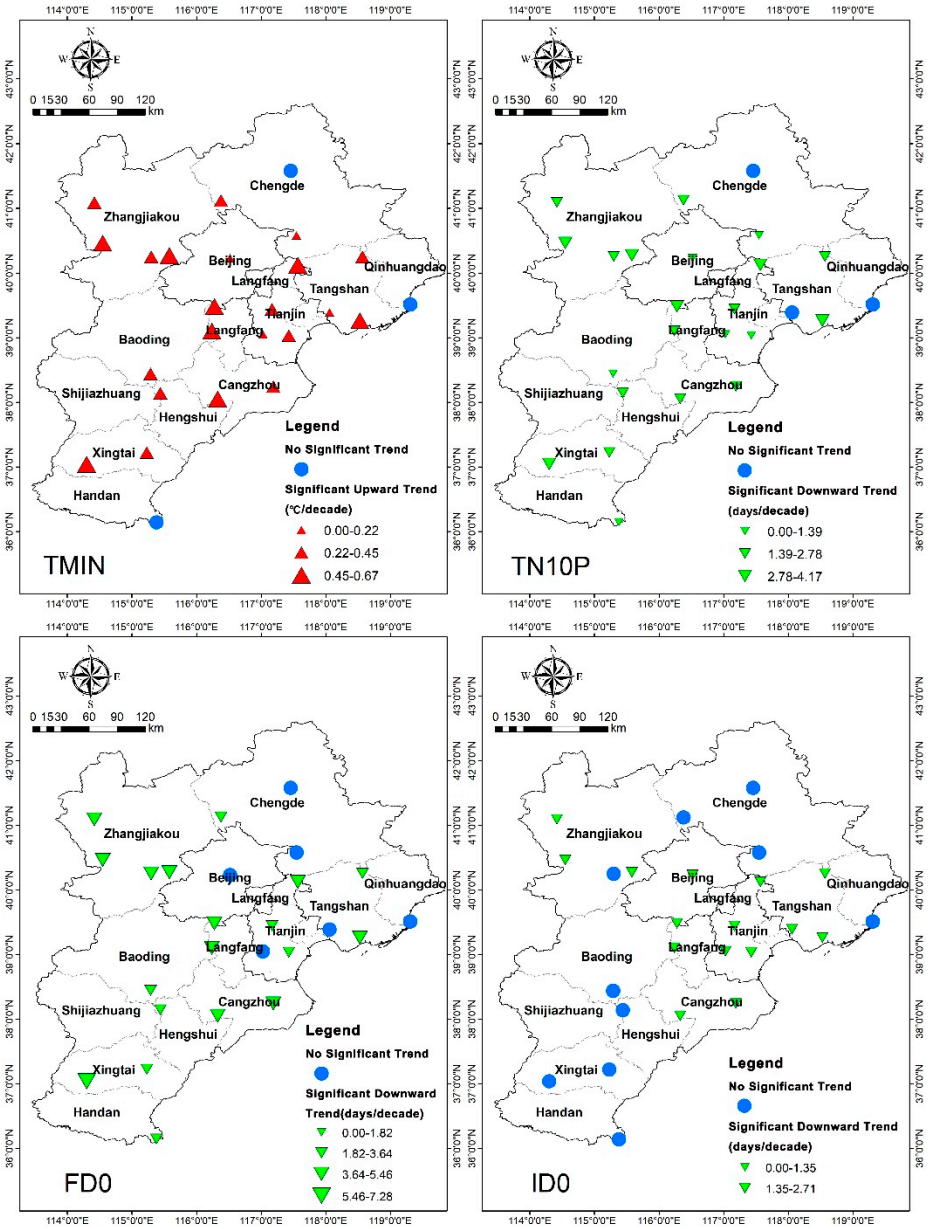

Figure 10. Spatial distributions of trends in indices representing cold weather extreme events for the meteorological stations in the Beijing–Tianjin–Hebei Region from 1959 to 2018. NB: TMIN, the annual minimum temperature; TN10P, the annual count of days when TMIN was <the 10th percentile; FD0, the annual count of days when TMAX was <0 °C; and ID0, the annual count of days when TMIN was <0 °C.

4. Discussion

At a regional scale, our results show that intensity, accumulated amount, and the frequency of extreme precipitation events per year decreased in the BTHR. In the Haihe Basin, which encompasses most of the BTHR, Du et al. have also reported decreasing trends in extreme precipitation [10]. This coincides with the findings of our study. Chu et al., Wang et al., and Yan et al. have revealed that flood season precipitation has decreased on both a regional and local scale [29–31]. As the occurrence of extreme precipitation events usually overlaps with the flood season in the BTHR, their results also support our findings. Our results show that the trends in most extreme precipitation indices at many stations were not statistically significant, although a few stations showed significant decreasing trends. This suggests that the mechanisms driving the occurrence of extreme precipitation events are

very complex. The BTHR is adjacent to the Bohai Sea, which is in the Pacific Ocean; therefore, its precipitation is greatly influenced by the East Asian summer monsoon [32]. Meanwhile, the rapid coordinated development of the Beijing–Tianjin–Hebei region and urbanization processes, which have brought urban-related warming, vertical wind motion, and changes to local moisture fluxes, have also influenced precipitation in the BTHR [33]. Although our long-term analysis of the frequency and magnitude of extreme precipitation events did not show significant increases, effective countermeasures need to be prepared for low-frequency but high-damage urban flood disasters, such as the event that happened on July 21, 2012, in Beijing, in which the precipitation within one day was over 460 mm. Therefore, to better forecast extreme precipitation events in this region, a numerical model considering the effects of urbanization on the water cycle and changes to the East Asian summer monsoon is needed. A successful model must consider all important human forces in detail [34]. For the BTHR, land use change related to urbanization needs to be effectively modeled, as how it disturbs the climate system will become more significant in the near future [35,36].

Our results indicate that both the daily maximum and minimum temperature have increased significantly in the BTHR. The magnitude of increase in the daily minimum temperature was larger than that of the daily maximum temperature. This is consistent with the findings of Wang et al. (their analysis of the Huang–Huai–Hai River Basin in China from 1961 to 2014, which included the BTHR) [37]. The indices related to hot weather extreme climate events showed significant increasing trends in the middle and north of the BTHR, including stations in two metropolises (Beijing and Tianjin) and their surrounding areas. Because several researchers have reported that heat waves are a great threat to human health [38,39], policymaking to protect public health should consider extreme hot weather. However, in the south of the BTHR, most trends were not significant for hot temperature events. This may be because irrigation is intense in the southern BTHR, and this has a significant cooling effect on the daily maximum temperature, which partially offsets the effect of urbanization [40]. Clearly, the cooling effects of cropland cannot be ignored [41]. At most stations, the daily minimum temperature and the indices of frequency of extreme cold weather events significantly increased and decreased, respectively. On the basis of simulations using the Community Land Model (CLM4.5), Lin et al. revealed that urban-related warming contributes more in winter in the BTHR, implying that urbanization is one of the underlying reasons for the decreasing trend in extreme cold weather events in this region [42]. The trend analyses of both extreme hot and cold weather events were influenced by changes in the regional surface energy balance, which are caused by anthropogenic activities. Therefore, more reasonable city planning that reduces anthropogenic heat release is necessary in the BTHR.

It should be noted that in situ observational data from meteorological stations is very accurate and has the longest temporal coverage in the BTHR, but it is limited by overall spatial coverage. In order to justify our results (described above), the trends of four indices representing the intensity and frequency of extreme precipitation events (i.e., RX1DAY, RX5DAY, R20mm, and R50mm) were also analyzed using two remote sensing gridded datasets: the Tropical Rainfall Measuring Mission 3B42 Daily dataset (TRMM, spatial resolution of 0.25°, available at https://pmm.nasa.gov/data-access/downloads/trmm) and the Global Precipitation Climatology Project (GPCP, spatial resolution of 1°, available at https://www.ncdc.noaa.gov/cdr/atmospheric/precipitation-gpcp-daily). Remote sensing observations can capture more detail in terms of spatial heterogeneity than can scattered meteorological station data, while their accuracy is lower. Considering the temporal convergence of satellite observations, a comparison was made for the period from 1998 to 2018 (Figures 11 and 12). For the two intensity indices, the trends detected from the ground observations and from the two satellite datasets were all insignificant throughout the majority of the BTHR. The TRMM data seemed to detect more spatial variation than did the GPCP data, for which the spatial resolution was too coarse for the study area. Significant increasing trends were detected in some areas of the BTHR in all three datasets. However, the distributions of these areas were different. The consistencies of the detected trends in the frequency indices in the datasets were higher. All three datasets showed that the trends of R50mm were insignificant in most areas of the BTHR. For R20mm, trends in more than two-thirds and half of

the stations were similar to the trends of the corresponding grids in the TRMM and GPCP datasets, respectively. These findings indicate that the trends detected among the three datasets were generally similar for extreme precipitation events on a regional scale, showing that the trends detected from the meteorological station data were reasonable. Meanwhile, the differences in trends detected from the three datasets indicated that the accuracy of satellite observations needs to be improved to trace the magnitude of extreme precipitation events, using ground measurements for correction [43,44].

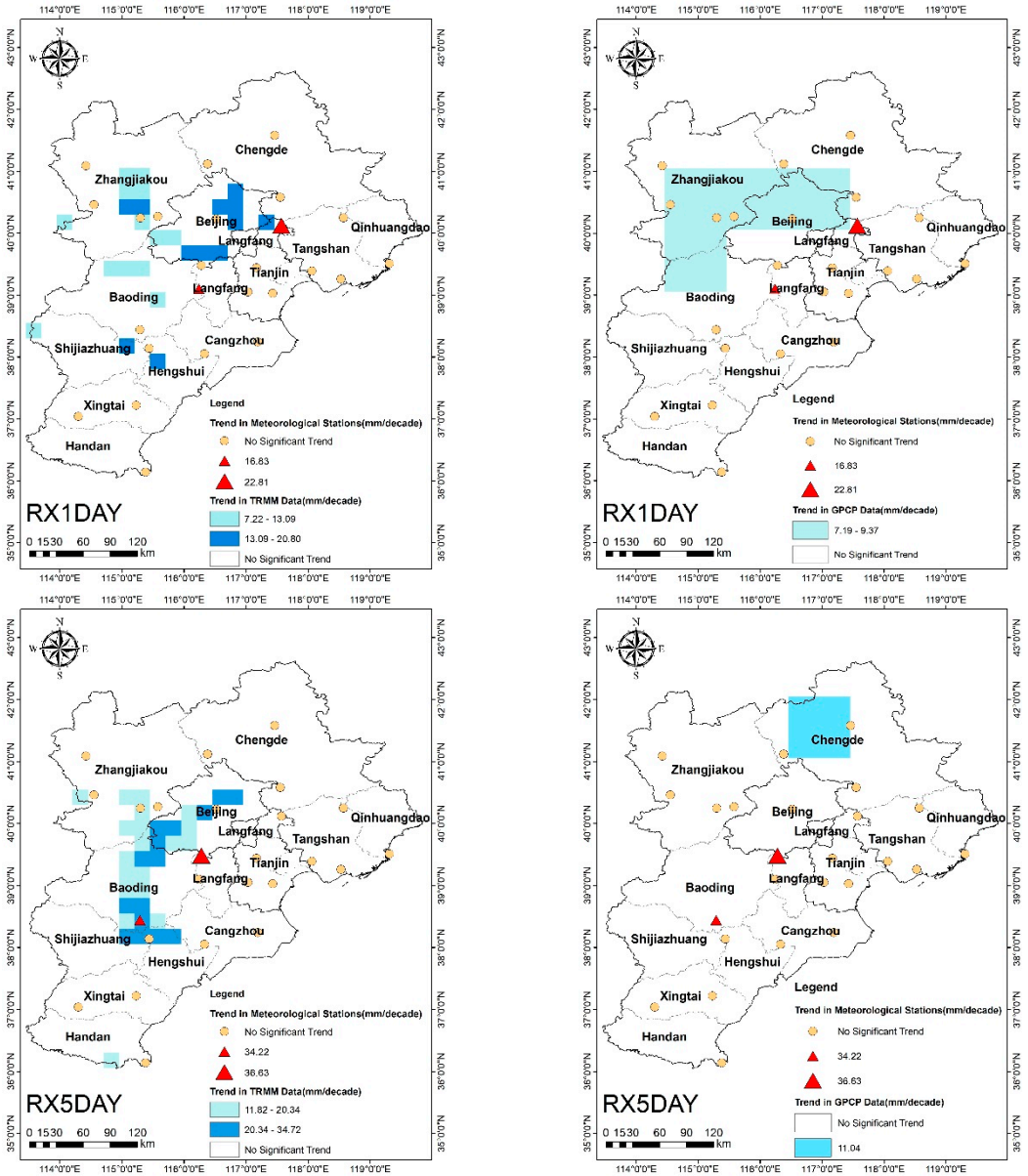

Figure 11. Spatial distributions of significant trends in indices representing the intensity of extreme precipitation events derived from ground measurement data from meteorological stations and satellite measurement data from the Tropical Rainfall Measuring Mission (TRMM) and the Global Precipitation Climatology Project (GPCP) for the Beijing–Tianjin–Hebei region from 1998 to 2018. NB: RX1DAY, the annual maximum daily precipitation; RX5DAY, the annual maximum consecutive five-day precipitation.

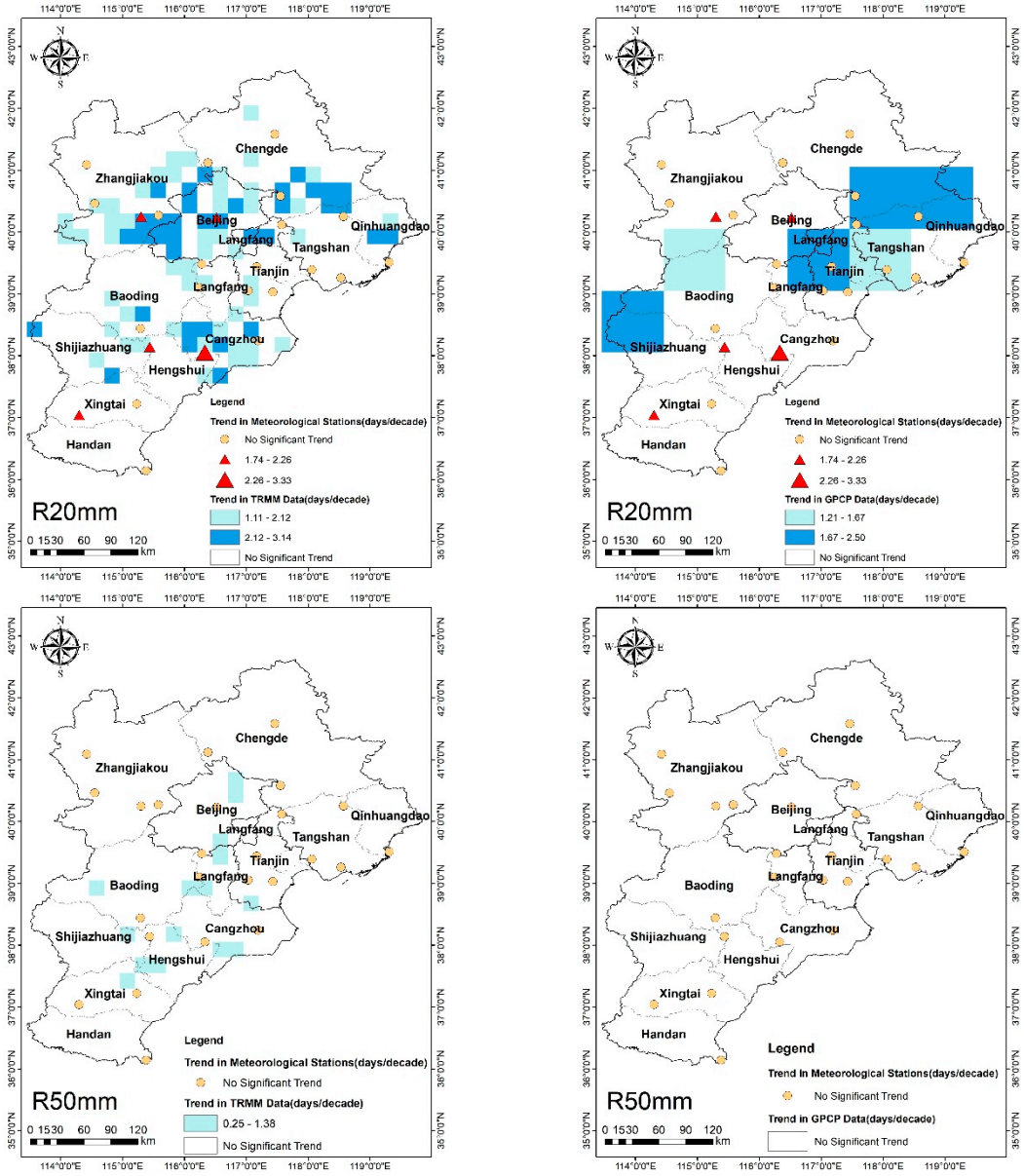

Figure 12. Spatial distributions of significant trends in indices representing the frequency of extreme precipitation events derived from ground measurement data from meteorological stations and satellite measurement data from the Tropical Rainfall Measuring Mission (TRMM) and the Global Precipitation Climatology Project (GPCP) for the Beijing–Tianjin–Hebei Region from 1998 to 2018. NB: R20mm, the annual count of days when daily precipitation was >20 mm; R50mm, the annual count of days when daily precipitation was >50 mm.

5. Conclusions

Understanding the characteristics and trends in extreme weather events is important for the sustainable development of regions with high population densities. With a long dataset encompassing the past six decades (1959–2018), the trends in extreme precipitation and temperature events were explored for the BTHR. Maximum one- and five-day precipitation and the accumulated amount of extreme precipitation per year showed decreasing trends on a regional scale. The number of days that precipitation was greater than 50 mm and the maximum number of consecutive wet days decreased. For many stations, the above-mentioned indices did not change significantly over the past six decades. Only a limited number of stations showed significant decreasing trends. Both the maximum and

minimum temperatures showed significant increasing trends, indicating that the BTHR warmed up. However, the spatial distributions of the trends of indices related to the degree and frequency of extreme hot and cold weather events were different, which could have been caused by the variable effects of irrigation and urbanization on the regional surface energy balance. The knowledge gained from this study is valuable for water resource management, for developing more effective countermeasures for extreme weather events, and for more reasonable urban planning within the BTHR as well as in other highly populated arid and semiarid regions worldwide.

Author Contributions: W.S., J.Y., and Z.T. designed the idea and methodology; R.T. and Q.H. collected and processed the original data; R.T. and Q.H. did the analysis; R.T. and W.S. wrote the paper. All authors have read and agreed to the published version of the manuscript.

Funding: This study was supported by the National Key R&D Program of China (Grant No. 2016YFC0401308), the National Natural Science Foundation of China (Grant No. 41671018), the Major Science and Technology Program for Water Pollution Control and Treatment (Grant No. 2018ZX07110006), and the 111 Project (B18006).

Conflicts of Interest: The authors declare no conflicts of interest.

References

1. Easterling, D.R.; Evans, J.L.; Groisman, P.Y.; Karl, T.R.; Kunkel, K.E.; Ambenje, P. Observed Variability and Trends in Extreme Climate Events: A Brief Review. *Bull. Am. Meteorol. Soc.* **2000**, *81*, 417–425. [CrossRef]
2. Lassa, J.; Teng, P.; Caballero, A.M.; Shrestha, M.R. Emergency Food Reserve Policy and Practice under Disaster and Extreme Climate Events. *Int. J. Disaster Risk Sci.* **2019**, *10*, 1–13. [CrossRef]
3. Solow, A.R. On Detecting Ecological Impacts of Extreme Climate Events and Why It Matters. *Philos. Trans. R. Soc. B Biol. Sci.* **2017**, *372*, 1723. [CrossRef] [PubMed]
4. Kevin, E.T.; John, T.F.; Theodore, G.S. Attribution of Climate Extreme Events. *Nat. Clim. Chang.* **2015**, *5*, 725–730.
5. Begueria, S.; Angulo-Martinez, M.; Vicente-Serrano, S.M.; Lopez-Moreno, J.I.; El-Kenawy, A. Assessing Trends in Extreme Precipitation Events Intensity and Magnitude Using Non-stationary Peaks-over-threshold Analysis: A Case Study in Northeast Spain from 1930 to 2006. *Int. J. Climatol.* **2011**, *31*, 2102–2114. [CrossRef]
6. Grotjahn, R.; Black, R.; Leung, R.; Wehner, M.F.; Barlow, M.; Bosilovich, M.; Gershunov, A.; Gutowski, W.J.; Gyakum, J.R.; Katz, R.W.; et al. North American Extreme Temperature Events and Related Large Scale Meteorological Patterns: A Review of Statistical Methods, Dynamics, Modeling, and Trends. *Clim. Dyn.* **2016**, *46*, 1151–1184. [CrossRef]
7. Alexander, L.V.; Zhang, X.; Peterson, T.C.; Caesar, J.; Gleason, B.; Klein Tank, A.M.G.; Haylock, M.; Collins, D.; Trewin, B.; Rahimzadeh, F.; et al. Global Observed Changes in Daily Climate Extremes of Temperature and Precipitation. *J. Geophys. Res. Atmos.* **2006**, *111*, D05109. [CrossRef]
8. Diffenbaugh, N.S.; Singh, D.; Mankin, J.S.; Horton, D.E.; Swain, D.L.; Touma, D.; Charland, A.; Liu, Y.J.; Haugen, M.; Tsiang, M.; et al. Quantifying The Influence of Global Warming on Unprecedented Extreme Climate Events. *Proc. Natl. Acad. Sci. USA* **2017**, *114*, 4881–4886. [CrossRef]
9. Choi, G.; Collins, D.; Ren, G.Y.; Trewin, B.; Baldi, M.; Fukuda, Y.; Afzaal, M.; Pianmana, T.; Gomboluudev, P.; Huong, P.T.T.; et al. Changes in Means and Extreme Events of Temperature and Precipitation in the Asia-Pacific Network Region, 1955-2007. *Int. J. Climatol.* **2009**, *29*, 1906–1925. [CrossRef]
10. Du, H.; Xia, J.; Zeng, S.D.; She, D.X.; Liu, J.J. Variations and Statistical Probability Characteristic Analysis of Extreme Precipitation Events Under Climate Change in Haihe River Basin, China. *Hydrol. Process.* **2014**, *28*, 913–925. [CrossRef]
11. Soltani, M.; Laux, P.; Kunstmann, H.; Stan, K.; Sohrabi, M.M.; Molanejad, M.; Sabziparvar, A.A.; SaadatAbadi, A.R.; Ranjbar, F.; Rousta, I.; et al. Assessment of Climate Variations in Temperature and Precipitation Extreme Events over Iran. *Theor. Appl. Climatol.* **2016**, *126*, 775–795. [CrossRef]
12. Kao, L.S.; Chiu, Y.H.; Tsai, C.Y. An Evaluation Study of Urban Development Strategy Based on of Extreme Climate Conditions. *Sustainability* **2017**, *9*, 284. [CrossRef]
13. Fan, J.A.; Sun, W.C.; Zhao, Y.; Xue, B.L.; Zuo, D.P.; Xu, Z.X. Trend Analyses of Extreme Precipitation Events in the Yarlung Zangbo River Basin, China Using a High-Resolution Precipitation Product. *Sustainability* **2018**, *10*, 1369. [CrossRef]

14. Harris, R.M.B.; Beaumont, L.J.; Vance, T.R.; Tozer, C.R.; Remenyi, T.A.; Perkins-Kirkpatrick, S.E.; Mitchell, P.J.; Nicotra, A.B.; McGregor, S.; Andrew, N.R.; et al. Biological Responses to the Press and Pulse of Climate Trends and Extreme Events. *Nat. Clim. Chang.* **2018**, *8*, 579–587. [CrossRef]
15. Han, Z.Y.; Shi, Y.; Wu, J.; Xu, Y.; Zhou, B.T. Combined Dynamical and Statistical Downscaling for High-Resolution Projections of Multiple Climate Variables in the Beijing-Tianjin-Hebei Region of China. *J. Appl. Meteorol. Climatol.* **2019**, *58*, 2387–2403. [CrossRef]
16. Zhang, J.; Sun, F.B.; Liu, W.B.; Liu, J.H.; Wang, H. Spatio-temporal Patterns of Drought Evolution over the Beijing-Tianjin-Hebei Region, China. *J. Geogr. Sci.* **2019**, *29*, 863–876. [CrossRef]
17. Wang, J.H.; Jiang, D.; Huang, Y.H.; Wang, H. Drought Analysis of the Haihe River Basin Based on GRACE Terrestrial Water Storage. *Sci. World J.* **2014**. [CrossRef]
18. Zhang, S.; Huang, G.; Qi, Y.J.; Jia, G.S. Impact of Urbanization on Summer Rainfall in Beijing–Tianjin–Hebei Metropolis under Different Climate Backgrounds. *Theor. Appl. Climatol.* **2018**, *133*, 1093–1106. [CrossRef]
19. Zhao, N.; Yue, T.X.; Li, H.; Zhang, L.L.; Yin, X.Z.; Liu, Y. Spatio-temporal Changes in Precipitation over Beijing-Tianjin-Hebei Region, China. *Atmos. Res.* **2018**, *202*, 156–168. [CrossRef]
20. Zhang, Y.; Huang, G.H.; Wang, X.Q.; Liu, Z.P. Observed Changes in Temperature Extremes for the Beijing-Tianjin-Hebei Region of China. *Meteorol. Appl.* **2017**, *24*, 74–83. [CrossRef]
21. Wang, X.L.; Feng, Y. RHtestsV4 User Manual; Climate Research Division, Atmospheric Science and Technology Directorate, Science and Technology Branch, Environment Canada: 2013. Available online: http://etccdi.pacificclimate.org/software.shtml (accessed on 1 July 2013).
22. Wang, X.L. Accounting for Autocorrelation in Detecting Mean-shifts in Climate Data Series Using the Penalized Maximal t or F Test. *J. Appl. Meteor. Climatol.* **2008**, *47*, 2423–2444. [CrossRef]
23. Wang, X.L. Penalized Maximal F-test for Detecting Undocumented Mean-shifts without Trend-change. *J. Atmos. Ocean. Technol.* **2008**, *25*, 368–384. [CrossRef]
24. Zhang, P.F.; Ren, G.Y.; Xu, Y.; Wang, X.L.; Qin, Y.; Sun, X.B.; Ren, Y.Y. Observed Changes in Extreme Temperature over the Global Land Based on a Newly Developed Station Daily Dataset. *J. Clim.* **2019**, *32*, 8489–8509. [CrossRef]
25. Wang, X.H.; Wang, B.T.; Xu, X.Y. Effects of Large-scale Climate Anomalies on Trends in Seasonal Precipitation over the Loess Plateau of China from 1961 to 2016. *Ecol. Indic.* **2019**, *107*. [CrossRef]
26. Zhai, Y.Z.; Guo, Y.L.; Zhou, J.; Guo, N.; Wang, J.S.; Teng, Y.G. The Spatio-temporal Variability of Annual Precipitation and its Local Impact Factors during 1724–2010 in Beijing, China. *Hydrol. Process.* **2014**, *28*, 2192–2201. [CrossRef]
27. Wang, B.; Xu, Z.X. Spatial and Temporal Variations of Precipitation in Haihe River Basin in the Recent 53 years, Remote Sensing and GIS for Hydrology and water resources. In Proceedings of the 3rd Remote Sensing and Hydrology Symposium (RSHS 14)/3rd International Conference of GIS/RS in Hydrology, Water Resources and Environment (ICGRHWE 14), Guangzhou, China, 24–27 August 2014.
28. Sen, P.K. Estimates of the Regression Coefficient Based on Kendall's tau. *J. Am. Stat. Assoc.* **1968**, *63*, 1379–1389. [CrossRef]
29. Chu, J.T.; Xia, J.; Xu, C.Y.; Li, L.; Wang, Z.G. Spatial and Temporal Variability of Daily, Precipitation in Haihe River Basin, 1958–2007. *J. Geogr. Sci.* **2010**, *20*, 248–260. [CrossRef]
30. Wang, Z.G.; Luo, Y.Z.; Liu, C.M.; Xia, J.; Zhang, M.H. Spatial and Temporal Variations of Precipitation in Haihe River Basin, China: Six Decades of Measurements. *Hydrol. Process.* **2011**, *25*, 2916–2923. [CrossRef]
31. Yan, T.Z.; Shen, Z.Y.; Bai, J.W. Spatial and Temporal Changes in Temperature, Precipitation, and Streamflow in the Miyun Reservoir Basin of China. *Water* **2017**, *9*, 78. [CrossRef]
32. Luo, Y.Z.; Wang, Z.G.; Liu, X.M.; Zhang, M.H. Spatial and Temporal Variability of Precipitation in Haihe River Basin, China: Characterization and Management Implications. *Adv. Meteorol.* **2014**. [CrossRef]
33. Song, X.M.; Zhang, J.Y.; AghaKouchak, A.; Sen Roy, S.; Xuan, Y.Q.; Wang, G.Q.; He, R.M.; Wang, X.J.; Liu, C.S. Rapid Urbanization and Changes in Spatiotemporal Characteristics of Precipitation in Beijing Metropolitan Area. *J. Geophys. Res. Atmos.* **2014**, *119*, 11250–11271. [CrossRef]
34. Pielke, R.A.; Mahmood, R.; McAlpine, C. Land's Complex Role in Climate Change. *Phys. Today* **2016**, *69*, 40–46. [CrossRef]
35. Woldemichael, A.T.; Hossain, F.; Pielke, R.; Beltran-Przekurat, A. Understanding the Impact of Dam-Triggered Land Use/Land Cover Change on the Modification of Extreme Precipitation. *Water Resour. Res.* **2012**. [CrossRef]

36. Pielke, R.A.; Adegoke, J.; Beltran-Przekurat, A.; Hiemstra, C.A.; Lin, J.; Nair, U.S.; Niyogi, D.; Nobis, T.E. An Overview of Regional Land use and Land cover Impacts on Rainfall. *Tellus Ser. B Chem. Phys. Meteorol.* **2007**, *59*, 587–601. [CrossRef]
37. Wang, G.; Yan, D.H.; He, X.Y.; Liu, S.H.; Zhang, C.; Xing, Z.Q.; Kan, G.Y.; Qin, T.L.; Ren, M.L.; Li, H. Trends in Extreme Temperature Indexes in Huang-Huai-Hai River Basin of China during 1961–2014. *Theor. Appl. Climatol.* **2018**, *134*, 51–65. [CrossRef]
38. Song, X.P.; Wang, S.G.; Li, T.S.; Tian, J.H.; Ding, G.W.; Wang, J.X.; Wang, J.X.; Shang, K.Z. The Impact of Heat Waves and Cold Spells on Respiratory Emergency Department Visits in Beijing, China. *Sci. Total Environ.* **2018**, *615*, 1499–1505. [CrossRef]
39. Zhang, J.; Li, T.T.; Tan, J.G.; Huang, C.R.; Kan, H.D. Impact of Temperature on Mortality in Three Major Chinese Cities. *Biomed. Environ. Sci.* **2014**, *27*, 485–496. [CrossRef]
40. Shi, W.J.; Tao, F.L.; Liu, J.Y. Regional Temperature Change over the Huang-Huai-Hai Plain of China: The Roles of Irrigation Versus Urbanization. *Int. J. Climatol.* **2014**, *34*, 1181–1195. [CrossRef]
41. He, Y.Q.; Lee, E.; McNeil, B.; Meng, L.; Warner, T.; Zégre, N. Impacts of Land Use and Land Cover Change on Regional Climate in China. *Environ. Res. Lett.* **2019**. [CrossRef]
42. Lin, S.; Feng, J.M.; Wang, J.; Hu, Y.H. Modeling the Contribution of Long-term Urbanization to Temperature Increase in Three Extensive Urban Agglomerations in China. *J. Geophys. Res. Atmos.* **2016**, *121*, 1683–1697. [CrossRef]
43. Huang, C.C.; Zheng, X.G.; Tait, A.; Dai, Y.J.; Yang, C.; Chen, Z.Q.; Li, T.; Wang, Z.L. On Using Smoothing Spline and Residual Correction to Fuse Rain Gauge Observations and Remote Sensing Data. *J. Hydrol.* **2014**, *508*, 410–417. [CrossRef]
44. Choubin, B.; Khalighi-Sigaroodi, S.; Mishra, A.; Goodarzi, M.; Shamshirband, S.; Ghaljaee, E.; Zhang, F. A Novel Bias Correction Framework of TMPA 3B42 Daily Precipitation Data Using Similarity Matrix/Homogeneous Conditions. *Sci. Total Environ.* **2019**, *694*, 133680. [CrossRef] [PubMed]